

Improved direct detection of low-energy ions using a multipixel photon counter coupled with a novel scintillator

Benjamin Winter², Simon J. King¹, Mark Brouard², and Claire Vallance^{1,a}

¹*Department of Chemistry, University of Oxford, Chemistry Research Laboratory, 12 Mansfield Rd, Oxford OX1 3TA*

²*The Department of Chemistry, University of Oxford, The Physical and Theoretical Chemistry Laboratory, South Parks Road, Oxford, OX1 3QZ, United Kingdom.*

^a*e-mail: claire.vallance@chem.ox.ac.uk*

Abstract

Recently, we described a direct low-energy ion detector for time-of-flight applications based on a single-photon avalanche diode (SPAD) array optically coupled to an LYSO (cerium-doped lutetium yttrium orthosilicate) scintillator. Here we present a greatly improved version of the detector, developed through testing of a number of different scintillator and phosphor materials in combination with a commercially-available SPAD array. The various scintillator materials have been characterized in terms of the achievable detection sensitivity and time response when used in conjunction with the SPAD array. Organic para-polyphenylene dyes, a relatively new class of scintillator for particle detection, were found to exhibit markedly improved performance relative to well-established scintillators such as LYSO crystal scintillators and P47 phosphors, both in terms of brightness and time response. The optimized detector has a time resolution of ~ 2 ns, an improvement of more than an order of magnitude over the original version, at the same time as achieving a five to ten-fold improvement in detection sensitivity. Our approach points the way towards the development of a generic silicon-based ion detector technology to complement or replace the microchannel-plate (MCP) ion detectors in widespread use at present. Such a detector would remove the need for high voltages and high vacuum, and at the same time greatly reduce detector cost relative to MCP-based detectors.

1. Introduction

The ability to measure the arrival time of a charged particle with high sensitivity and high precision is a key experimental requirement in many areas of chemistry and physics. Detectors with such capabilities are required in areas ranging from gas-phase reaction dynamics^{1,2} and particle physics³ to medical imaging⁴. However, perhaps the largest area of application is time-of-flight (ToF) mass spectrometry, in which precise and accurate arrival time measurements must be made for ions accelerated to energies of up to 20 keV.

In addition to exhibiting high sensitivity and time resolution, an ideal ToF detection system should have a high saturation threshold, a mass-independent response, and be sufficiently robust to resist damage under a range of operating conditions. Low maintenance requirements and/or replacement costs are also desirable. The simplest ToF detectors rely on direct charge detection at a Faraday cup or plate. While offering universal detection for particles of any mass, the ion currents recorded are generally at the sub-femtoampere to picoampere level, yielding low sensitivity. This is true even with substantial amplification, which is often achieved at the expense of time resolution. More commonly, the detector is comprised of a particle multiplier or one or more microchannel plates (MCPs)^{5,6}. An ion incident on such a detector elicits a cascade of electrons, yielding a signal amplification of several orders of magnitude. For example, one of the most commonly-used detector configurations comprises a pair of microchannel plates mounted in a chevron arrangement, and

yields a charge amplification of around 10^6 . The readout system for an MCP-based detector typically consists either of a metal anode coupled to a fast current amplifier, or (particularly for imaging experiments) a phosphor screen coupled either to a photomultiplier and associated amplification electronics or to a CCD or CMOS camera. The intrinsic response speed of a microchannel plate is on the order of 100 ps or less⁷, and this has been realised in a number of cases, but the overall time response of an MCP detector is often limited either by the time response of the amplification electronics or by the decay lifetime of the phosphor if one is present⁸.

Despite the fact that MCP-based detectors have become the standard in ToF mass spectrometry, they suffer from a number of shortcomings. They are both expensive and extremely fragile, a less than ideal combination. Reliable operation is only possible at pressures below 10^{-5} mbar or so, with operation at higher pressures resulting in electrical arcing that can cause catastrophic damage to the plates. They also have a maximum output current⁹, which sets a limit on data acquisition rates at the level of around 10^8 - 10^9 counts $\text{cm}^{-2} \text{s}^{-1}$. Finally, the secondary electron emission from the MCPs does not scale linearly with the kinetic energy of the detected particles, but instead scales with their velocity¹⁰. In ToF mass spectrometry this has the consequence that because the ion velocity scales as the square root of the mass, the detection efficiency decreases with increasing ion mass. This effect can be mitigated to a reasonable extent by the use of suitable discrimination and pulse-counting electronics, so that the recorded signal depends only on the number of recorded ion events rather than on the intensity of the signals they generate. However, at some point the intensities of the signal peaks generated by the MCPs at very high ion masses will fall below the discriminator threshold, and detection will therefore fail.

High-energy charged particles (MeV or higher) are readily detected using a combination of a scintillator and a photomultiplier tube. In the past, this has not been a practical approach to the detection of much lower energy (0-10 keV) particles, due to the very low conversion efficiency of scintillators in this energy range. Low energy ions are stopped within the first few nanometers of the scintillator surface, generating only a handful of photons per keV, and yielding signals that are too small to be useful. However, the relatively recent development of silicon detectors capable of single-photon detection have made solid-state direct ion detectors an avenue worthy of further exploration. In particular, the development of in-pixel single-photon avalanche diodes (SPADs) opens up the intriguing possibility of single-photon-sensitive imaging detectors.

Recently, we reported a first prototype of a direct ion detection system¹¹, comprising an LYSO ($\text{Lu}_{1.8}\text{Y}_{0.2}\text{SiO}_5(\text{Ce})$) scintillator crystal coupled to a commercially-available SPAD array detector. The detector was used to record ToF mass spectra for butanone and carbon disulphide, and the response of the sensor was characterized as a function of ion kinetic energy, showing a linear increase that reflected the expected photon-emission characteristics of the LYSO scintillator. The work represented a very promising stepping stone on the path towards a generic silicon-based ion detector which would remove the need for high voltages and high-vacuum and at the same time greatly reduce detector cost relative to MCP-based detectors. However, the prototype detector exhibited relatively low detection sensitivity, and the time resolution was limited by the ~ 40 ns decay lifetime of the LYSO scintillator.

In the present work, we test a number of alternative scintillator materials, and show that by taking advantage of recently-developed fast scintillator screen materials¹², we are able to improve both the detection sensitivity and the time resolution of the direct ion detector by around an order of magnitude.

2. Experimental

The prototype detector and time-of-flight mass spectrometer used in the characterization experiments have been described in detail in earlier publications^{11,13}. The sensing element in the detector is a Hamamatsu multi-pixel photon counting sensor (MPPC S10362-11-025C), comprising a 1 mm^2 , 1600-pixel array of single-photon avalanche photodiodes (SPADs) arranged on a $25 \text{ }\mu\text{m}$ pixel pitch. The individual SPADs are connected together in parallel, such that the sensor

output is the sum of the individual pixel outputs. At present, individual pixels cannot be addressed independently, so imaging experiments are not possible and the sensor simply records the total incident photon signal. The sensor is most sensitive to photons in the wavelength range from 390 to 470 nm, with maximum sensitivity at ~420 nm. To create the direct ion detector, the MPPC sensor is optically coupled to a scintillator material. In the original experiments¹¹ this was a 1.5 x 1.5 x 0.2 mm³ LYSO scintillator crystal, mounted onto the front face of the sensor with a small amount of optical grease. In the present work, we have tested a number of different scintillator materials. These allow both the sensitivity and timing precision of the detector to be tuned. The intrinsic timing precision of the SPAD array is on the order of 200 ps, with a reset time for each pixel of around 20 ns, but the time resolution of the complete detector will in general be limited by the decay lifetime of the scintillator material.

In addition to repeating measurements with an LYSO scintillator for comparison with our previous study¹¹, the detector was tested with Exalite 389, Exalite 404, BBOT (2,5-Di-(5-tert-butyl-2-benzoxazolyl)-thiophene), P47, and Coumarin 503 scintillators. The performance of several of these scintillator materials in an MCP/scintillator-based particle imaging detector has been discussed in detail in a previous publication by the present authors¹². In the MCP-based detector, the Exalite scintillators in particular were found to outperform P47, exhibiting higher brightness and improved time resolution. None of these scintillators are available as single crystals, and instead they were prepared as thin layers on microscope cover slips, which were then attached to the front face of the MPPC sensor using a small amount of optical grease. The cover slips were 0.5 mm in thickness, and were cut to dimensions in line with that of the LYSO crystal. Thin layers were prepared using one of two different approaches¹², depending on the chemical and physical properties of the scintillator material.

Exalite 389, Exalite 404, and BBOT were deposited on the substrate by vacuum sublimation. The substrate was mounted on the cold finger of a commercially-available vacuum sublimation apparatus (Ace vacuum sublimation apparatus, inner diameter 60 mm), and 0.1 g of the scintillator material was placed in the base of the apparatus. The cold finger was filled with a water/ice slush, the apparatus was placed on a hot plate, and the scintillator material was then heated to the onset of sublimation at a pressure of 15 mbar until all of the material had sublimed and deposited on the surface of the cold finger. After complete sublimation, a layer of scintillator approximately 200 μm ($\pm 10\%$) in thickness, as measured with a micrometer, had formed on the substrate.

P47 (95% of particles < 7.2 μm) and Coumarin 503 scintillator screens were prepared via a sedimentation process. The substrates were placed in a beaker tilted at an angle of around 8°. A solution of barium chloride (1.16 mM in deionized water) was added to the beaker until the substrates were submerged beneath 5 cm of solution. 0.15 g of the scintillator was suspended in a 0.37 M potassium silicate solution and slowly poured into the prepared the beaker with the substrates. After a sedimentation period of 20 minutes the solution was siphoned from the beaker and the coated substrates were dried in an oven at 60°C for 20 minutes. This method yielded a layer thickness of approximately 350 μm ($\pm 10\%$), measured using a micrometer.

To interface with the mass spectrometer, the detector (MPPC with attached scintillator) was mounted on the vacuum side of a DN40 ConFlat flange, and connected to its control module (Hamamatsu C10507-11-025U MPPC control module) outside the vacuum via a six-pin electrical feedthrough. USB interface software provided by the manufacturer was used for data acquisition, with the option of viewing and acquiring either the analogue or digitized (photon counted) signal from the sensor. All experiments reported here utilized the analogue output. This was viewed and recorded using a fast digital oscilloscope (LeCroy DDA-260).

To produce an ion signal with which to characterize the detector, a pulsed molecular beam containing the sample molecule of interest was generated by supersonic expansion of the sample gas mixture through a Parker Hannifin Series 7 pulsed solenoid valve. After passing through a skimmer, the molecular beam was intersected either by a focused 193 nm laser beam from a Neweks PS100 excimer laser (10 Hz rep rate, 10 ns pulse width, 2.5 mJ pulse energy) or by a focused beam of 118 nm radiation. The 118 nm radiation is the 9th harmonic of a Nd:YAG laser (Continuum Surelite I, 10 Hz rep rate, 5

ns pulse width, 50 mJ pulse energy at 355 nm), generated by frequency tripling the fundamental in suitable non-linear crystals and then focusing the resulting 355 nm beam into a gas cell containing a phase-matched mixture of 24 mbar of Xenon and 325 mbar of Argon¹⁴. The molecular beam and laser beam cross within an electrostatic lens, which accelerates the resulting ions along a ~60 cm flight tube to the detector. Acceleration potentials in the range from 2 kV to 10 kV were used in the present work. These operating conditions are very similar to those employed when operating the mass spectrometer with a conventional MCP/P47 phosphor ion detector, with the exception that higher molecular beam fluxes were employed in order to compensate for the much smaller size of the SPAD-based sensor (1 mm² active area) relative to the MCP detector (40 mm active diameter). Mass spectra were typically acquired over 400 time-of-flight cycles.

Butanone and acetone were used as the sample molecules for the present work, and were ionized at 193 nm and 118 nm, respectively. The former was prepared as a mixture of 5% butanone in 1 bar of helium. The latter was prepared by bubbling helium at a pressure of 1050 mar through liquid acetone. Measurements made previously using a conventional MCP-based ion imaging detector have demonstrated that the bubbler method yields a near constant flux (to within 10%) of parent acetone ions over a prolonged period (>48 hours). This was confirmed by recording and comparing mass spectra for acetone at various points during the characterization process, and in particular at the beginning and end of the complete set characterization measurements. The mass spectra were found to be virtually indistinguishable.

The constant flux source described above allows us to make reliable measurements of the relative sensitivity of detectors equipped with various different phosphors. We also aimed to determine the time resolution achievable when employing the most promising scintillator material.

3. Results and Discussion

3.1 *Relative detection sensitivity*

The relative detection sensitivities of direct ion detectors employing Exalite 389, Exalite 404, BBOT, LYSO, P47, and Coumarin 503 scintillators are shown in Figure 1, as determined from the integrated peak areas of selected peaks in the time-of-flight mass spectra of acetone. Two sets of data are shown, in panels (a) and (b) respectively, corresponding to the $m/z = 58$ parent peak of acetone and the $m/z = 116$ dimer peak. The data are normalized to the signal for the $m/z=116$ mass peak recorded using an LYSO scintillator at an acceleration potential of 10 kV. The Exalite 389 scintillator is seen to outperform the others by some margin, yielding signal intensities more than a factor of two higher than the next highest contender, Exalite 404, and a factor of six or so higher than LYSO, the scintillator used in the previously-reported prototype detector¹¹. P47 performs around 50% better than LYSO on signal intensity, while BBOT and Coumarin 503 fare worse by around 20% and 70%, respectively. In all cases, the signal intensity shows an almost linear dependence on the ion acceleration potential, with some indications of the onset of signal saturation at the highest energies for the brighter scintillators. None of the scintillators showed any signs of degradation over the several-week time frame of these studies. It is interesting to note that while Exalite 389 clearly outperforms Exalite 404 in the direct detection of 1-10 keV ions, when Exalite 404 and Exalite 389 scintillators have been used previously to detect electrons in the energy range from 1 to 3 keV emitted from a pair of microchannel plates, the reverse was found to be true¹². It should also be noted that while the ion flux employed in the present experiments is up to an order of magnitude higher than that employed in the previously-reported¹² characterization of the various scintillator materials with a MCP/scintillator detector, the active area of the SPAD-based sensor is over a thousand times smaller, making it difficult to perform a direct quantitative comparison of the relative detection sensitivity of the two types of detector. When operating at similar ion fluxes to those employed in the MCP/scintillator-based measurements, signal was observed by the SPAD-based detector at the higher acceleration potentials (>6 kV), but in order to achieve a similar signal-to-noise ratio for the two types of detector, higher ion fluxes were required. As SPAD pixel technology improves and larger pixel arrays become available, it will become possible to

carry out a more direct comparison between the performance of direct SPAD-based ion detectors and that of conventional MCP-based detectors.

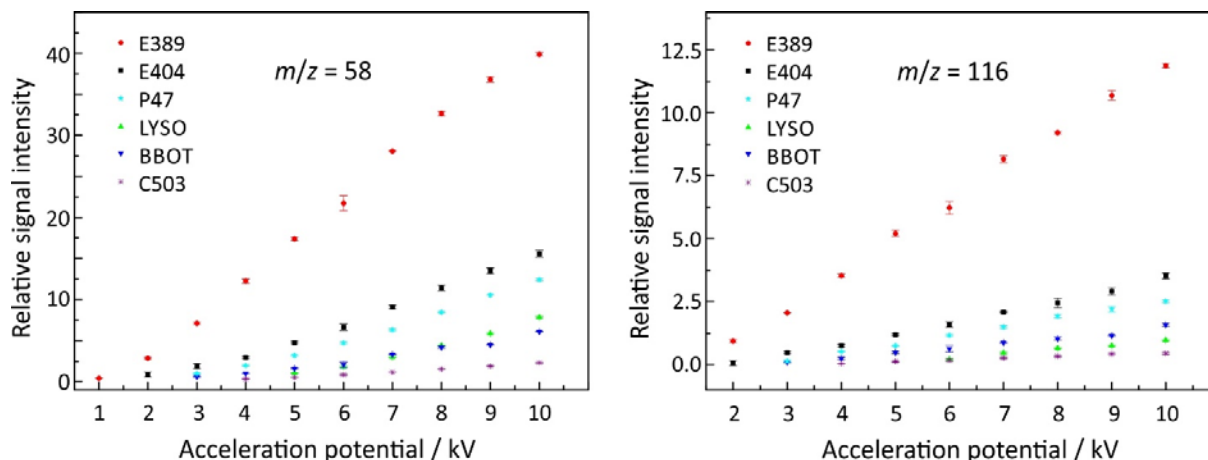


Figure 1: Relative detection efficiencies for detectors employing the various different scintillators, as a function of ion acceleration potential. The data are normalized to the signal for the $m/z=116$ mass peak recorded using an LYSO scintillator at an acceleration potential of 10 kV, and the error bars represent one standard deviation of the repeated measurements. The data plotted on the left were recorded for the $m/z = 58$ parent ion peak of acetone; those in the plot on the right were recorded for the $m/z = 116$ acetone dimer peak.

At present it is not possible to quantify the absolute detection efficiency of the direct ion detector. This would require a measurement of the absolute number of emitted photons per incident ion. However, the fact that all 1600 pixels in the MPPC sensor are connected in parallel means that it is not possible to isolate individual ion events given typical ion fluxes in our mass spectrometer. As noted in the Experimental section, great care was taken to ensure a constant flux of ions in order to ensure the reliability of the relative sensitivity measurements presented above.

In Figure 2, a ToF spectrum of butanone recorded using the direct ion detector with an Exalite 389 scintillator is compared with the corresponding data for the LYSO scintillator used in our original prototype direct ion detector¹¹. The two spectra were recorded under identical conditions, with interchange of the scintillators between measurements. The improvement in performance is clear, with the Exalite scintillator yielding a much more intense signal with greatly improved time resolution. Several mass spectra for acetone are shown in Figure 3, illustrating the improved detector performance for a number of different ion acceleration potentials. Note that the most intense peak, corresponding to the parent ion, shows evidence of saturation at the highest acceleration potentials, broadening and reducing in intensity relative to other peaks, and that care should be taken to avoid this by tuning the acceleration potential or other experimental parameters when using the detector in quantitative studies. The issue of saturation is a limitation imposed by the readout system for the MPPC sensor. Only a limited number of photons can be read out at any one time, severely limiting the number of SPAD pixels that can be activated simultaneously before saturation effects become evident. Several research groups are currently developing SPAD arrays in which each pixel can be addressed independently¹⁵; the availability of such detectors will immediately overcome this issue.

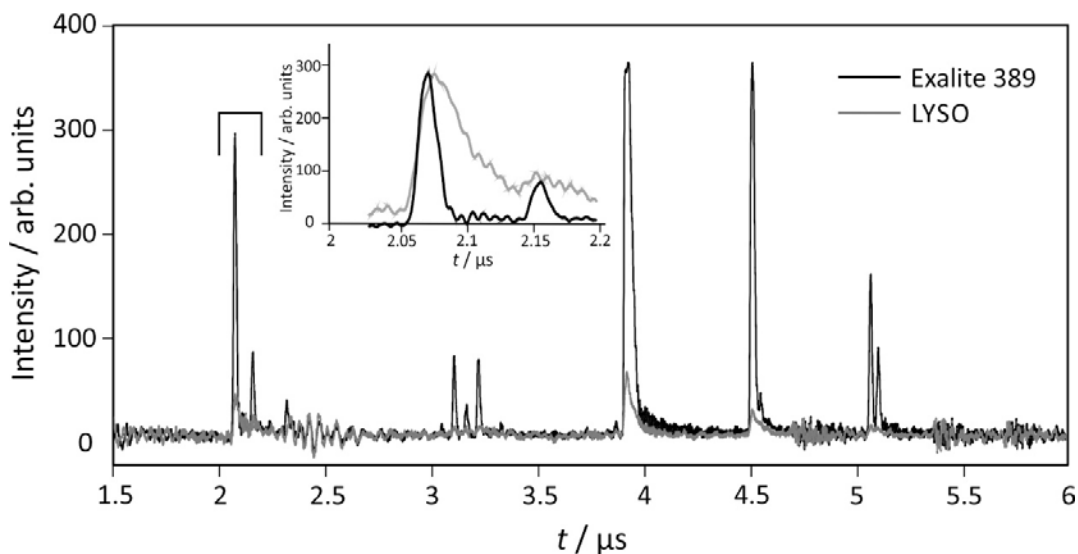


Figure 2: Comparison between ToF spectra of butanone recorded using a direct ion detector equipped with an Exalite 389 screen and with an LYSO screen. Spectra were recorded at an acceleration potential of 10 kV. The inset shows a small section of the time-of-flight spectrum near 2 μ s, illustrating the greatly improved time response of the Exalite 389 scintillator relative to the LYSO scintillator. The LYSO signal has been scaled in intensity and high-frequency noise has been partially filtered in order to aid the comparison.

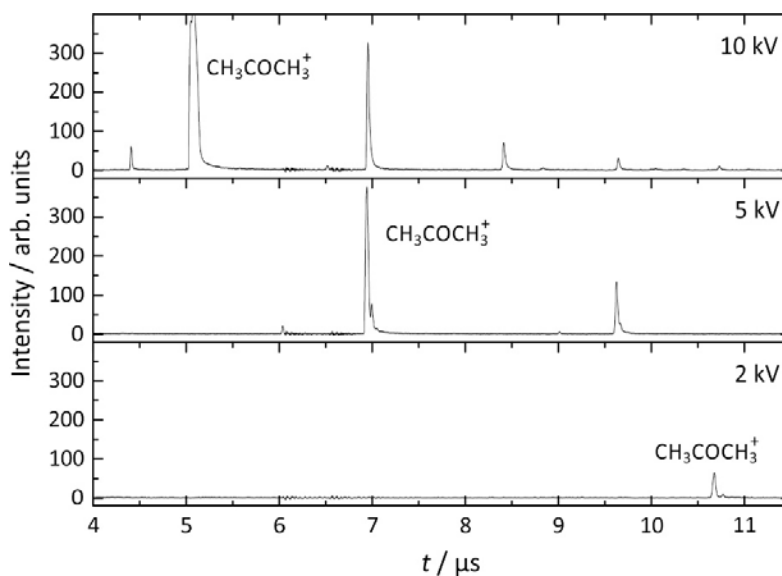


Figure 3: Time-of-flight spectra of acetone recorded with an Exalite 389 scintillator as a function of acceleration potential.

3.2 Time resolution

The intrinsic time resolution of the MPPC sensor is around 200 ns, implying that the limiting factor in the overall time resolution of the direct ion detector is likely to be the emission lifetime of the scintillator material. In our previous publication in which a prototype detector employing an LYSO scintillator was introduced, this was very evidently the case, with each mass peak in the recorded mass spectra exhibiting an exponentially decaying ‘tail’ with a lifetime matching the known ~ 40 ns emission lifetime of LYSO. To compare the performance of LYSO and an Exalite scintillator in this regard, the inset to Figure 2 shows two adjacent time-of-flight peaks near $m/z=12$ in the spectrum of butanone. The two signals

have been normalized to the maximum in the $m/z=12$ peak. The LYSO signal shows the expected exponential tail on each of the two peaks. In contrast, the Exalite 389 signal is much more Gaussian in shape, with a full-width-half-maximum of 16 ns. This is much longer than the emission lifetime of Exalite 389, implying that the resolution of our time-of-flight measurement in these experiments is no longer limited by the detector, but instead by the intrinsic resolution of the mass spectrometer. The electrostatic lens in our instrument is optimized for velocity-map imaging rather than for traditional Wiley-McLaren time-of-flight focusing, and as such achieves only a modest time-of-flight resolution. Also, ions are formed in the interaction region over a period of 5-10 ns, determined by the pulse length of the ionizing laser. The overall measured time resolution of ~ 16 ns results from a convolution of these two factors, and is in line with the prediction of ion trajectory simulations of our instrument carried out using the SIMION8.0 software package¹⁶.

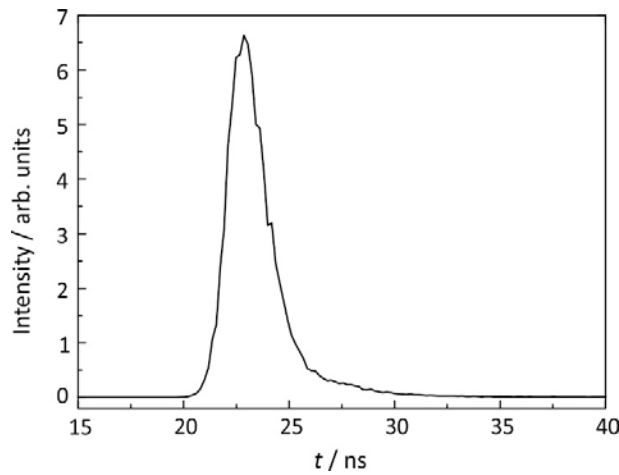


Figure 4: Fluorescence signal recorded for crystalline Exalite 404 scintillator following excitation at 337 nm. The decay time constant was determined to be 1.58 ± 0.03 ns.

Since the time resolution of the detector cannot be determined directly in our mass spectrometer, we can estimate the resolution based on emission lifetime measurements on Exalite dye screens following optical excitation. Previous work¹² on Exalite scintillators has indicated that the emission lifetimes following collisional excitation and photoexcitation are similar. We have characterized the emission lifetime of an Exalite 404 screen as part of an earlier study in which the screens were used to detect electrons emitted from microchannel plate detectors. The prepared screen was mounted in a Horiba Scientific Fluoromax 4 fluorescence spectrometer and the emission lifetime was measured following photoexcitation at 337 nm. A typical emission decay signal, recorded at an emission wavelength of 450 nm, is shown in Figure 4. Emission measurements at other wavelengths in the emission band yield very similar data. Taking appropriate account of the excitation pulse shape, the emission can be fitted well by a single exponential function with a decay constant of 1.58 ± 0.03 ns. Though we did not have the opportunity to make measurements for an Exalite 389 screen, the lifetime is expected to be similar. The measured lifetime is similar to the 1.5-2.0 ns pulse width of the LED used as the photoexcitation source, but at least place an upper bound on the scintillator emission lifetimes, and therefore the expected time resolution of the direct ion detector.

4. Conclusion

We have shown that by taking advantage of recent developments in scintillator screen technology, both the detection sensitivity and time resolution of a direct ion detector based on a commercial MPPC sensor can be improved by almost an order of magnitude. A performance comparison across a number of different scintillators indicates that Exalite-based

scintillator screens provide the highest brightness and time resolution when coupled to an MPPC sensor. Silicon-based direct ion detectors of this type hold considerable promise as robust, low-cost, high-performance detectors for mass spectrometry and other particle time-of-flight experiments, overcoming a number of limitations associated with microchannel-plate based detectors. A number of research groups around the world are currently developing pixelated SPAD arrays for imaging applications, in which each pixel is independently addressable. In addition to overcoming the issues of saturation associated with parallel readout of pixels, as discussed earlier, coupling such an array with a suitable scintillator material will lead to a new generation of MCP-free high performance particle imaging detectors. Such detectors will remove the requirement for high vacuum in ion imaging measurements, opening the way to new directions in mass spectrometer and other instrument design, as well as offering improved time resolution and ion throughput relative to existing detectors.

Acknowledgements

The authors would like to thank Dr. Daniel Pooley, STFC Rutherford Appleton Laboratory, for use of the fluorescence spectrometer and assistance with fluorescence lifetime measurements, and Andrei Nomerotski for his contribution to developing the original LYSO-based detector. The work reported in this manuscript was supported by EPSRC Programme Grant EP/L005913/1. This work is the subject of patent applications by ISIS Innovations Ltd. (UK patent application numbers 1310476.5 and 1111915.3).

References

- 1 M. Ahmed, D. S. Peterka, and A. G. Suits, *Chem. Phys. Lett.*, 301(3-4), 372 (1999).
- 2 M. Brouard, E. K. Campbell, A. J. Johnsen, C. Vallance, W. H. Yuen, and A. Nomerotski, *Rev. Sci. Instrum.*, **79(12)**, 123115/1 (2008).
- 3 W. R. Leo, *Techniques for Nuclear and Particle Physics Experiments*, vol. 2nd Edition (Springer-Verlag, 1994).
- 4 W. W. Moses, *Nucl. Instruments Methods Phys. Res. Sect. A Accel. Spectrometers, Detect. Assoc. Equip.*, **580(2)**, 919 (2007).
- 5 D. W. Koppenaal, C. J. Barinaga, M. B. Denton, R. P. Sperline, G. M. Hieftje, G. D. Schilling, F. J. Andrade, and I. V Barnes James H., *Anal. Chem.*, **77(21)**, 418A (2005).
- 6 J. L. Wiza, *Nucl. Instruments Methods*, **162(1-3)**, 587 (1979).
- 7 J. Girard and M. Bolore," *Nucl. Instruments Methods*, **140(2)**, 279 (1977).
- 8 G. F. Knoll, *Radiation Detection and Measurement*, vol. 4th Edition (John Wiley & Sons, Inc, 2010).
- 9 W. B. Feller, *Nucl. Instrum. Methods Phys. Res. A*, **310**, 249 (1991).
- 10 M. Krems, J. Zirbel, M. Thomason, and R. D. DuBois, *Rev. Sci. Instrum.*, **76(9)**, 093305/1 (2005).

-
- 11 E. S. Wilman, S. H. Gardiner, A. Nomerotski, R. Turchetta, M. Brouard, and C. Vallance, *Rev. Sci. Instrum.*, **83(1)**, 013304/1 (2012).
 - 12 B. Winter, S. J. King, M. Brouard, and C. Vallance, *Rev. Sci. Instrum.*, **85(2)**, 023306 (2014).
 - 13 W. S. Hopkins, M. L. Lipciuc, S. H. Gardiner, and C. Vallance, *J. Chem. Phys.*, **135(3)**, 034308 (2011).
 - 14 A. H. Kung, J. F. Young, and S. E. Harris, *Appl. Phys. Lett.*, **22**, 301 (1973).
 - 15 See for example E. Charbon, M. Fishburn, R. Walker, R. K. Henderson, and C. Niclass, "SPAD-Based Sensors", in "TOF Range-Imaging Cameras", Ed. F. Remondino and D. Stoppa (Springer-Verlag Berlin Heidelberg, 2013, DOI 10.1007/978-3-642-27523-4_2) and references therein.
 - 16 SIMION8.0, Scientific Instrument Services, <http://www.simion.com>.